Molecular dynamics simulation of mechanical properties of carbon nanotube re-enforced celluloses

Kecheng Li
Western Michigan University
DEWEI Qi (dewei.qi@wmich.edu)
Western Michigan University

Research Article

Keywords:

Posted Date: June 7th, 2022

DOI: https://doi.org/10.21203/rs.3.rs-1734693/v1

Abstract

Cellulose, hemi-cellulose, lignin are major chemical components in wood paper. Various types of wet and dry strength additives are used to enhance optical and mechanical properties of recycled paper. One of possible materials is carbon nanotube. In order to explore probability of use of carbon nanotubes as re-enforcing materials and to understand how carbon nanotubes affect mechanical properties of paper, a single walled carbon nanotube is inserted into a I_β crystalline cellulose solid, its mechanical properties are studied by using energy minimization and molecular dynamics (MD) simulations. Based on the method, the crystals are stretched in axial direction at a constant speed and stress and strain are computed and recorded at atomic level. Our results show that carbon nanotube can significantly enhance mechanical properties of paper.

1. Introduction

In the paper industry, millions of tons of paper are recycled and reused in a recycling process to save energy and natural wood resource. One of problems that the paper industry faces today is that mechanical strength of recycled fibers is greatly weakened by contaminants and by previously intensive drying process [1, 2].

To improve the mechanical strength of recycled cellulose fibers, various types of drying or wet strength additives, at nano size scale, are mixed with cellulose fibers in paper making process. These strength additives include polyacrylamide, polyvinyl, polyamide, polyamide-epichlorohydrin, as well as different types of fillers. One of possible fillers or re-enforce materials is carbon nanotubes (CNT), which possess extremely high mechanical strength. It is possible that a small amount of CNT could be mixed with celluloses to achieve novel properties by combining properties from the two different constituents. In fact, it was found that the mechanical, chemical, electrical, optical, magnetic and electro- and magneto-optical properties of the CNTs have extensive applications in many different areas. For example, theoretical and experimental results reveal that the Youngs' modulus of CNTs could be as high as 1–5 TPa [3] and the tensile strength could be as high as 200 GPa [4]. Moreover, their aspect ratio is very large and diameter scale may be comparable with various cellulose chains. Thus, CNTs naturally suggest themselves for use as one component of composites to enhance the mechanical properties. Indeed, people experimentally studied the mechanical properties of polyimide/single-wall CNT composites [5]. They found that the storage modulus increased by 65% upon addition of 1% carbon NTs by volume [6]. Some authors simulated the stress-strain behavior of polyimide CNT composites by using molecular dynamics (MD) simulations and found that long carbon CNTs could significantly reinforce mechanical properties [7]. It suggests that celluloses mixed with carbon nanotubes may result in high mechanical properties.

In this work, atomistic modelling is used to investigate the stress-strain behavior of crystalline cellulose and its composites with single-walled CNT. We will focus on numerical simulations of the performance of composites of CNT re-enforced celluloses and on the evaluation of its improvement with respect to

mechanical properties. A series of MD simulations is conducted to study how CNT influence the mechanical properties of CNT-cellulose composites.

Our results show that CNT can significantly enhance the mechanical properties of cellulosic materials, which is potentially important for recycled paper.

Next section will briefly introduce molecular dynamics methods and construction of composite of CNT re-enforced celluloses. Section 3 presents simulation results of density, energies, and Youngs' modulus. Section 4 makes a conclusion.

2. Method

2.1 Crystalline cellulose

Celluloses can be presented in different crystalline phases as I_α, I_β, II and III_I. Native plant celluloses are mixture of I_α.and I_β. Their ratio of I_α to I_β depends on original fiber sources. In wood fibers, I_β is a major component and adapted in this simulation work.

First, I_β crystalline celluloses are built by using Cellulose Builder developed by Gomes and Skaf [8]. One β 1–4 linked D-glucose unit is shown in Fig. 1.

The simulated cellulose crystal has thirty-two chains, each chain with five repeated β 1–4 linked D-glucose units as shown in Fig. 2. The total atom number in this crystal is 7620, which are located in a parallelepiped box with a triclinic symmetry. The basis three vectors of the simulation box are **a**=(x, y, z)= (31.136, 0, 0), **b**=(-3.7135, 32.593, 0), and **c**=(0, 0, 51.90), respectively, where length unit is in Angstrom. The cellulose chains are along axial c- or z-direction. During simulations, periodical boundary conditions are imposed in all the three directions.

2.2 Composite of CNT re-enforced cellulose

In order to build a CNT-cellulose composite, one of cellulose chains is removed from the crystalline cellulose solid as shown in Fig. 3 (a) and replaced by a single walled carbon nanotube with $(n_1, n_2) =$ (3,3) structure as shown in Fig. 3 (b). The single walled carbon nanotube, as shown in Fig. 3. (c), has a diameter of 4.07 Angstrom, which is smaller than the size of space of the removed cellulose chain. The distance between its neighboring cellulose chains is 7.78 Angstrom. The single walled carbon nanotube is built by mapping the atoms of a 2D graphite to the surface of a cylinder. (n_1, n_2) denotes a particular scheme to build the nanotube from the 2D Bravais lattice of the graphite. The diameter of the carbon nanotube depends on the integer numbers of n_1 and n_2. More details can be found in White et. al. work [9]. Following their work, a carbon nanotube builder software was developed at Western Michigan University [7].

2.3 MD simulations

A open software of molecular dynamics simulation package called Lammps [10] is employed to simulate various physical properties, such as potential energy, total energy, density, hydrogen bond energy etc..

In simulations, the popular Charmm force fields [11] are adopted for cellulose. In Charmm force fields, total energy E_t in the cellulose system can be presented by

$$E_t(r) = \sum_{bonds} k_b(r - r_0)^2 + \sum_{UB} k_{UB}(s - s_0)^2 + \sum_{angle} k_a(\theta - \theta_0)^2 + \sum_{dihedrals} k_d(1 + \cos(n\phi - \phi_0) + \sum_{impropers} k_i(\psi - \psi_0)^2 + \sum_{vdw} \epsilon_{ij} \left[\left(\frac{R_{min,ij}}{r_{ij}}\right)^{12} - 2\left(\frac{R_{min,ij}}{r_{ij}}\right)^{6}\right] + \sum_{electrostatic} \frac{q_i q_j}{4\pi\epsilon_0 r_{ij}}$$

The first term in the right side of the equation represents the bonding energy, the second term is the energy contribution due to vibration of bonded two atoms (only Charmm force field has this term), the third term is the angular energy between two bonds, the fourth term stands for the dihedral energy, the fifth term is improper energy, the sixth term is Van der Waal nonbond potential energy, the last term is electric interaction energy. k_b, k_{UB}, k_a, k_d, k_i are the spring coefficients of corresponding terms; ϵ_{ij} is the depth of energy well of Lennard-Jones (LJ) potential; $R_{min,ij}$ is its minimum energy position; q_i is the charge of atom i; ϵ_0 is di-electrical constant; r_0, s_0, θ_0, ψ_0, and ψ_0 are corresponding equilibrium position or angles. Both the LJ and electric Coulombic forces are cut off at 12 Angstrom. From the gradient of total energy, the forces acting on each atom can be calculated. Then, based on the forces, a leap-frog algorithm is utilized to update velocities and positions of all atoms.

Carbon nanotubes have stable structure due to sp^2 hydride bonds, resulting in large mechanical strength. It is evident that the Tripos 5.2 force fields [12] are suitable for description of sp^2 bonds of carbon nanotube. This was verified by our previous work [7]. The Tripos 5.2 force fields are employed again for presenting carbon nanotube motion in this work.

Hydrogen bonds (H-bond) are critically important for stability of cellulose structure. The Dreiding model [13–14] is selected to track the hydrogen bonds. The distance between donor and acceptor is cut off at 4.5 Angstroms and the angle is cut off at 120 degrees in this three-body H-bond model.

In MD simulation, first, an energy minimization is imposed on all atoms, then they run in a NVT ensemble for 40000 time steps at a temperature of 298 K^0. Next, the system runs at a constant pressure of 1atm and at the same temperature for additional 260000 time steps, allowing the system to reach an equilibrium state. During the constant pressure run, 1atm pressure is kept in the x-, y-, and z- directions and a zero pressure is kept in the xy-, yz-, and xz-directions. The volume or density and different type of energies can be measured in the NPT time integration via Nose/Hoover algorithm [15–16]. One step time interval is 0.5 femtoseconds.

2.3 Stress and strain

Finally, the crystalline celluloses are stretched along the axial c- or z-direction of the crystal at the room temperature while 1 atm pressure is kept in the x- and y-directions. During stretching, one time step is in 0.25 femtosecond and stretching rate is at $\frac{0.000001}{femtosecond}$. Total time steps for stretching are 400000. The results of stress and strain are computed and recorded. Youngs modulus are evaluated from the slope of initial linear portion of the stress-strain curve. The same applies to the composite of CNT re-enforced cellulose.

3. Results

3.1 Density

In the NPT simulations, total number of atoms, temperature, and pressure are kept constants, volume is varied and computed, and density of the cellulose crystal is predicted. The results of density as a function of time step are plotted along with temperature in Fig. 4. It shows that after 200000 timesteps, the values of density and temperature are stable with small fluctuations, indicating that an equilibrium is arrived. The predicted average density of the cellulose nanocrystal is about 1.63 $\frac{g}{cm^3}$ in present work. Experimental results of density of I_β cellulose nanocrystal is 1.676 $\frac{g}{cm^3}$ reported by Nishiyama et. al. [17] and 1.625 $\frac{g}{cm^3}$ reported by Krassig [18]. Fernando et. al.[19] used a quantum mechanical density function to theoretically predict the density of 1.61 $\frac{g}{cm^3}$. It is clearly demonstrated that our simulation results are in an excellent agreement with others' experimental and numerical results. Figure 4 also shows that the average temperature is well controlled around 298 (K) as expected.

In addition, the results of density and temperature as a function of time step are reported in Fig. 5 for composite of CNT re-enforced cellulose. It is shown that the density of the composite is about 1.66 $\frac{g}{cm^3}$, slightly larger than that of pour cellulose. This reasonable result comes from more compacted structure of CNT, resulting in a denser structure of the composite, which can provide a larger mechanical strength.

3.2 Energies and Hydrogen bonds.

The simulation results of hydrogen-bond (H-bond), potential, and total energy as a function of time step are plotted in Fig. 6 for the I_β cellulose crystal.

All energies are stable in final stage of the run. The total hydrogen bond energy is about − 3100 Kcal/mol and the total potential energy is about − 16750 Kcal/mol. The ratio of the H-bond energy to the total potential energy is about 18.5%. No doubt, H-bonds cannot be ignored. From an energy point of view, H-bonds provide a lower energy to stabilize molecular structures, allow cellulose chains binding together, and devote large mechanical strength to the cellulose crystal.

In order to probe functions of H-bonds, simulations are carried out at the same conditions except that the H-bonds are removed. The simulation results of potential and total energies are compared between two cases with and without H-bonds in Fig. 7. It is shown that potential energy is lower in the case with H-bonds than in the case without H-bonds, so does the total energy.

So far, it is numerically verified that H-bonds can lower energy, allowing cellulose structure more stable. It is not surprised that the total energy is higher than the potential energy since kinetic energy contributes a positive energy as temperature.

The results of H-bond, potential and total energy against time steps are graphed in Fig. 8 for the composite of CNT re-enforced cellulose. It is noted that total H-bond binding energy of 2970 Kcal/mol in the composite is smaller than that of 3100 Kcal/mol in the pure cellulose crystal in comparison of reading between Figs. 8 and 6. This is caused by a lack of H-bonds between cellulose chains and CNT due to its hydrophobic surface. However, strong mechanical strength of CNT itself can offset the deficient. In next section, we turn our attention to mechanical properties.

3.3 Youngs' modulus

The purpose of present work is to use CNT to reinforce the mechanical properties of cellulose. Since the CNT is lied along the axial- or z-direction of cellulose, the stress $\sigma_{zz}$and Youngs' modulus in the re-enforced z-direction are our focus.

During stretching of crystalline in z- or axial direction, the stress in this direction is calculated and averaged over all atoms at each time step. The results of stress, averaged over every 100 steps, against strain are depicted and compared between the normal cellulose crystal and the cellulose crystal without H-bonds in Fig. 9.

The slopes of stress-strain curves at its initial portion represent the Youngs' modulus. Our simulation result of Youngs' modulus in axial direction is 150 GPa for I_β cellulose crystal. In literature, experimental values of Young's modulus have been determined by using different experimental techniques. For instance, x-ray diffraction measurements [20–24] of the axial elastic modulus measured along the longitudinal axis range from 90 to 150 GPa. An axial elastic modulus of 220 ± 50 GPa was also reported by Diddens *et al* [25]. Our result well agrees with the experimental values, evidencing that our method and

results are reliable. Figure 9 also compares the stress-stain curve of cellulose crystal with that of the cellulose without H-bonds. The slope of the curve is much larger for the cellulose than for the cellulose with H-bonds removed. The Youngs' modulus for later is 103 GPa, which is 31% lower than the normal cellulose. It is obviously illustrated that H-bonds play a critical role in contribution of mechanical strength.

Finally, the result of stress-strain curve is presented for the composite of CNT re-enforced cellulose and compared with that of cellulose crystal in Fig. 10.

The slopes of initial stress-strain curves are larger for composite of CNT re-enforced cellulose than for the pure cellulosic solid. The Youngs modulus increases from E = 150 GPa for the pure cellulose crystals to E = 195GPa for the composite of CNT re-enforced cellulose. This is a 30% increase by replacing a cellulose chain with a CNT although the mass weight fraction is only 2.8% increase in the CNT re-enforced celluloses, demonstrating that carbon nanotube can significantly re-enforce mechanical strength.

4. Conclusion

In this work, molecular dynamics simulation package Lammps is employed to simulate mechanical properties of I_β crystalline cellulose in NPT ensembles, where Charmm force fields are adopted. The predicted density and Youngs' modulus of crystalline celluloses from the simulations are in an excellent agreement with experimental results. Next, the H-bonds are intentionally removed from the same cellulose crystal, unfortunately, its Youngs' modulus reduces 31%, evidencing importance of H-bonds. Subsequently, one cellulose chain is replaced by a single walled carbon nanotube in the crystalline celluloses, the Youngs modulus increases 30%. It is demonstrated that CNT can dramatically enhance mechanical properties of the cellulosic system.

It is recommended that carbon nanotube should be modified to be hydrophilic for more H-bonds between cellulose chains and CNT surface.

Declarations

Acknowledge

We appreciate the financial support from US DOE (Project Award No. DE-EE0007897).

References

1. Jason Wang, Dewei Qi, Kecheng Li, "Identification and Characterization of Sticky Contaminants in Multiple Recycled Paper Grades", submitted to Celluloses, June 2022.
2. Xiuyu Liu, Yan Jiang, Xueping Sing, Chengrong Qin, Shuangfei Wang, Kecheng Li, "A bio-mechanical process for cellulose nanofiber production – Towards a greener and energy conservation solution", Carbohydrate Polymers 208(2019). DOI:10.1016/j.carbpol.2018.12.071
3. Overney G, Zhong W and Tomanek D 1993 *Z. Phys. D: At. Mol. Clusters* **27** 93

4. Meyyappan M and Han J 1998 *Prototype Tech. Int.* **6** 14
5. Park C, Ounaies Z,WatsonKA, Pawlowski K, Lowther S E, Connell JW, Siochi E J, Harrison J S and St Clair T L, “Polymer-single wall carbon nanotube composites for potential spacecraft applications”, NASA/CR-2002 211940 *ICASE Report* No 2002-36
6. Frankland S J V, Harik V M, Odegard G M, Brenner D W and Gates T S 2003 “The stress–strain behavior of polymer-nanotube composites from molecular dynamics simulation” *Compos. Sci. Technol.* **63** 1655–61
7. Dewei Qi, Jeffrey Hinkley and Gouwei He, “Molecular dynamics simulation of thermal and mechanical properties of polyimide–carbon-nanotube composites”, Modelling Simul. Mater. Sci. Eng. **13** (2005) 493–507, doi:10.1088/0965-0393/13/4/002
8. Thiago C. F. Gomes, Munir S. Skaf, “Cellulose-Builder: A toolkit for building crystalline structures of cellulose”, Journal of Computational Chemistry 2012, Volume 33, Issue 14, pages 1338-1346. DOI: 10.1002/jcc.22959
9. White C T, Robertson D H and Mintmire J W 1993 “Helical and rotational symmetries of nanoscale graphitic tubules” Phys. Rev. B 47 5485, DOI:https://doi.org/10.1103/PhysRevB.47.5485
10. Lammps Molecular Dynamics Simulation (https://www.lammps.org)
11. Martin Karplus, Michael Levitt and Arieh Warshel, for "the development of multiscale models for complex chemical systems”, were awarded Nobel Prize in Chemistry in 2013, PNAS, November 25, 110 (49) 19656-19657, https://doi.org/10.1073/pnas.1320569110
12. Clark M, Cramer R D C and Opedenbosch N V 1989 “Validation of the general purpose Tripos 5.2 force field” *J. Comp. Chem.* **10** 982–1012. **https://doi.org/10.1002/jcc.540100804**
13. Stephen L. Mayo, Barry D. Olafson, and William A. Goddard III, “DREIDING: a generic force field for molecular simulations (acs.org)”, J Phys Chem, 94, 8897-8909 (1990).
14. Liu, Bryantsev, Diallo, Goddard III, “PAMAM dendrimers undergo pH responsive conformational changes without swelling” J. Am. Chem. Soc 131 (8) 2798 (2009). https://Doi.org/10.1021/ja8100227
15. Nose S, “A unified formulation of the constant temperature molecular dynamics methods”, J. Chem. Phys. **81**, 511 (1984); https://doi.org/10.1063/1.447334
16. Hoover W G 1985 “Canonical dynamics: equilibrium phase space/distributions”, Phys. Rev. A 31 1695–7, https://doi.org/10.1103/PhysRevA.31.1695
17. Nishiyama, Y.; Langan, P.; Chanzy, H. “Crystal structure and hydrogen-bonding system in cellulose Iβ from synchrotron X-ray and neutron fiber diffraction”.J. Am. Chem. Soc. 2002, 124, 9074–9082, https://doi.org/10.1021/ja0257319
18. Krassig, H. A. “Cellulose: Structure, Accessibility and Reactivity”, Gordon and Breach Science Publishers: Yverdon, 1993; Vol. 11.
19. Fernando L Dri1, ShunLi Shang, Louis G Hector Jr, Paul Saxe, Zi-Kui Liu, Robert J Moon, and Pablo D Zavattieri “Anisotropy and temperature dependence of structural, thermodynamic, and elastic

properties of crystalline cellulose Iβ: a first-principles investigation", Modelling Simul. Mater. Sci. Eng. 22 (2014) 085012 (28pp). https://doi.org/10.1088/0965-0393/22/8/085012

20. Sakurada I, Nukushina Y and Ito T 1962, "Experimental determination of the elastic modulus of crystalline regions in oriented polymers" *J. Polym. Sci.* **57** 651–60. **https://doi.org/10.1002/pol.1962.1205716551**
21. Sakurada I, Ito T and Nakamae K 1964, "Elastic moduli of polymer crystals for the chain axial direction", *Die Makromol. Chem.* **75** 1–10. **https://doi.org/10.1002/macp.1964.020750101**
22. Matsuo M, Sawatari C, Iwai Y and Ozaki F 1990, "Effect of orientation distribution and crystallinity on the measurement by x-ray diffraction of the crystal lattice moduli of cellulose I and II", *Macromolecules* **23** 3266–75. Effect of orientation distribution and crystallinity on the measurement by x-ray diffraction of the crystal lattice moduli of cellulose I and II (acs.org)
23. Nishino T, Takano K and Nakamae K 1995 "Elastic modulus of the crystalline regions of cellulose polymorphs", *J. Polym. Sci.* B **33** 1647–51 **https://doi.org/10.1002/polb.1995.090331110**
24. Ishikawa A, Okano T and Sugiyama J 1997 "Fine structure and tensile properties of ramie fibres in the crystalline form of cellulose I, II, IIII and IVI", *Polymer* **38** 463–8. https://doi.org/10.1016/S0032-3861(96)00516-2
25. Diddens I, Murphy B, Krisch M and M¨uller M 2008 "Anisotropic elastic properties of cellulose measured using inelastic x-ray scattering",*Macromolecules* **41** 9755–9, https://doi.org/10.1021/ma801796u

Figures

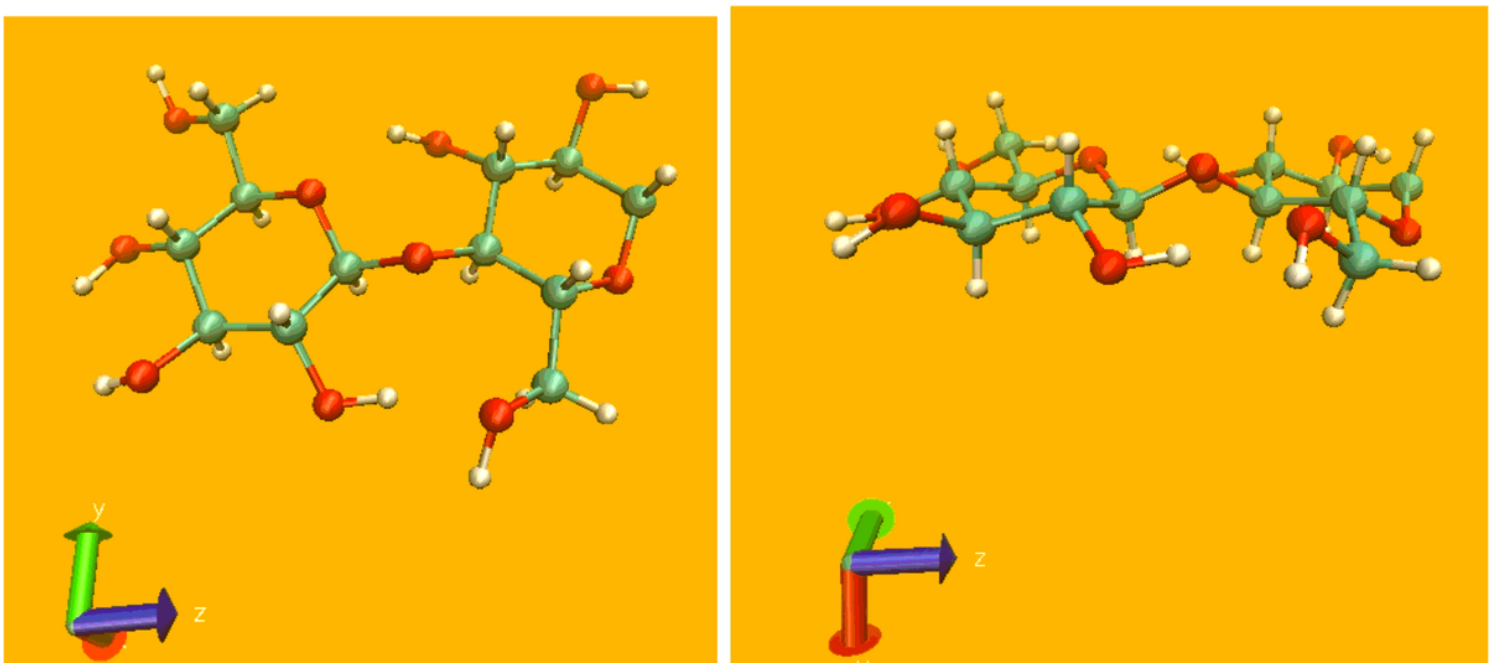

Figure 1

one β 1-4 linked D-glucose unit is shown in a chaired structure. The left and right pictures represent the view in different directions. Carbon atoms are green-colored, oxygen atoms are red-colored, and hydrogen atoms are white-colored.

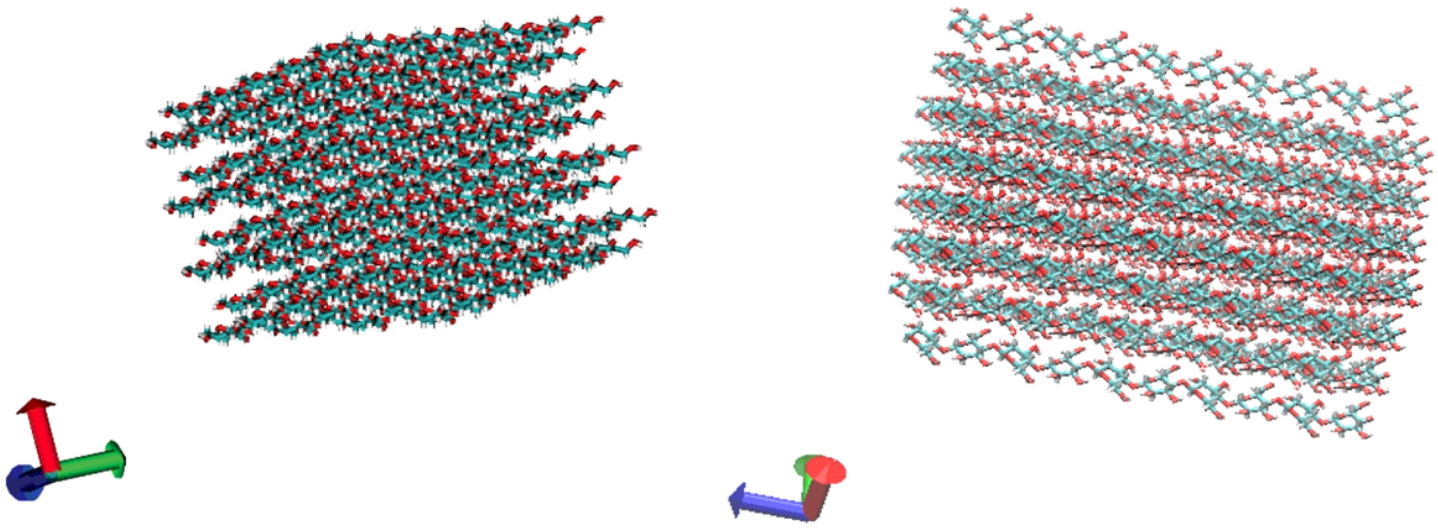

Figure 2

The simulated crystalline celluloses have thirty-two cellulose chains, each with five-repeated β 1-4 linked D-glucose unit. They are viewed in different directions.

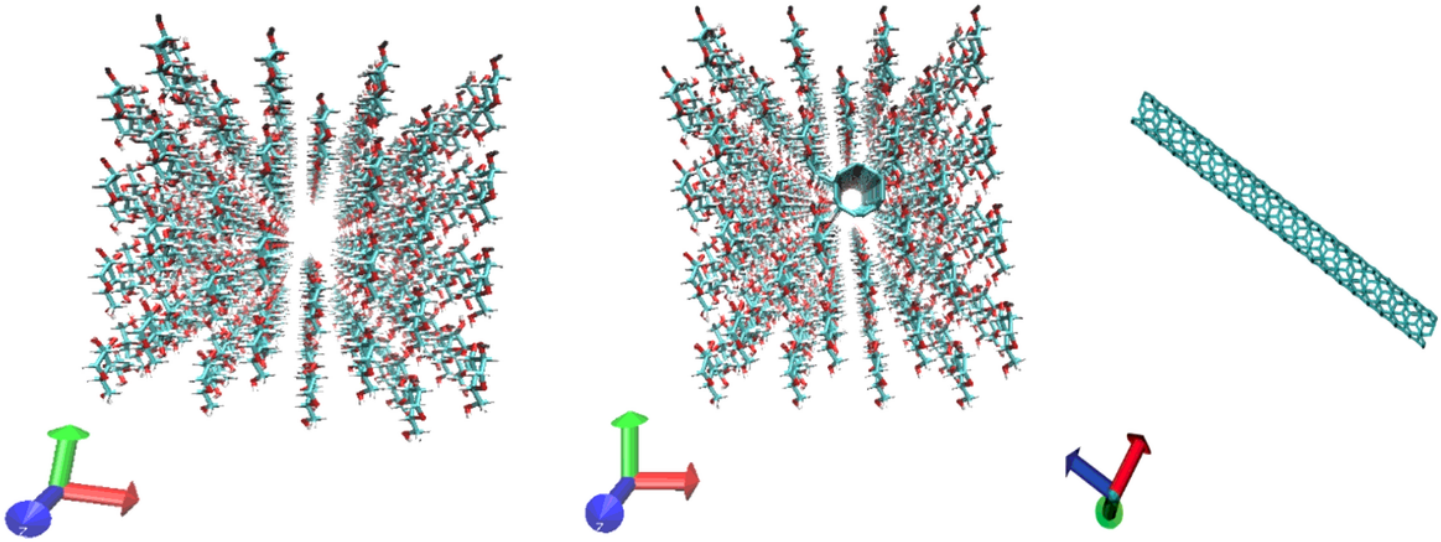

Figure 3

a) crystalline celluloses with one chain removed (left); b) a single walled carbon nanotube is inserted into the crystal (center); c) a (3,3) carbon nanotube (right).

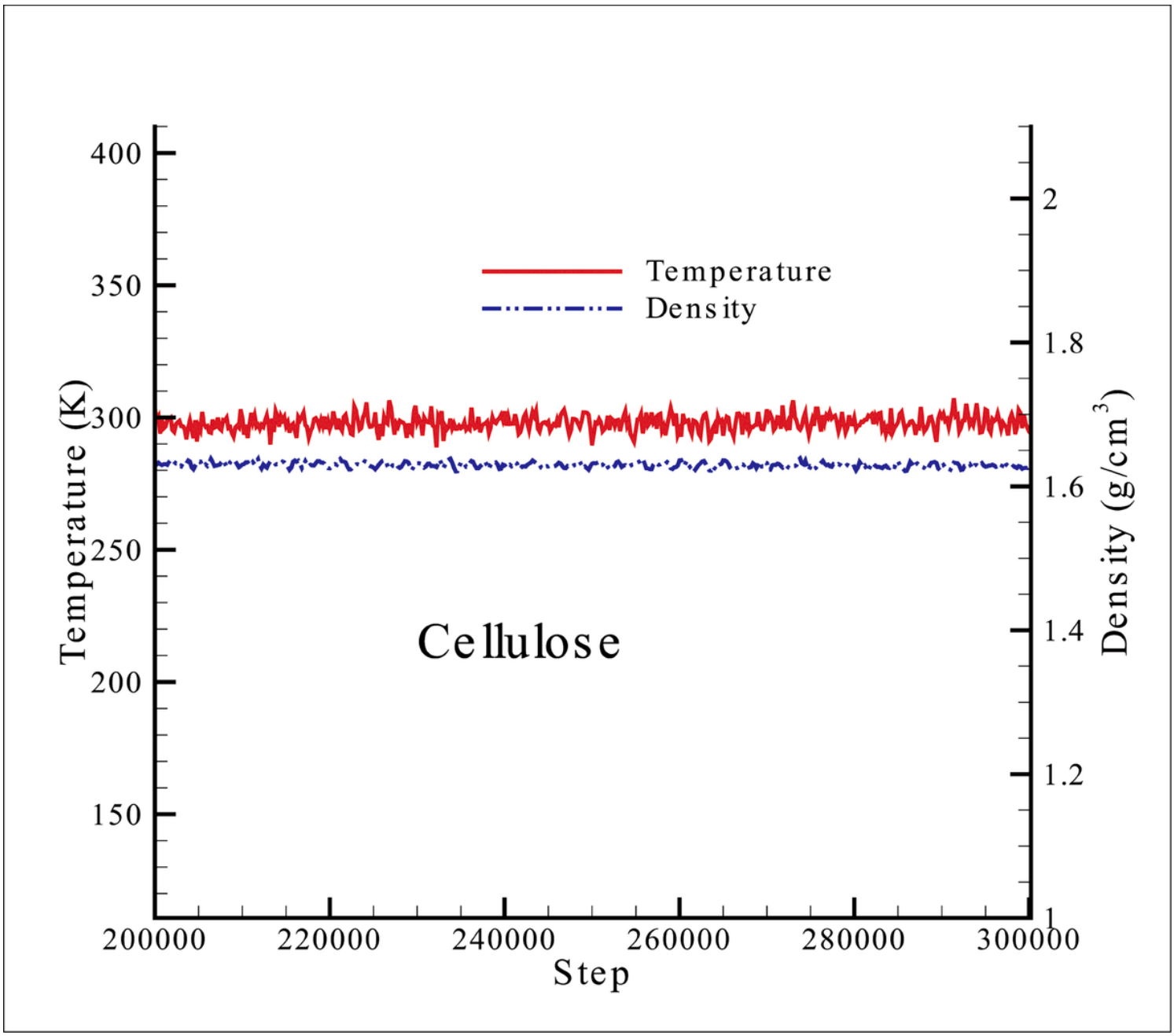

Figure 4

The simulation results of density and temperature as a function of time step are plotted for I_β cellulose.

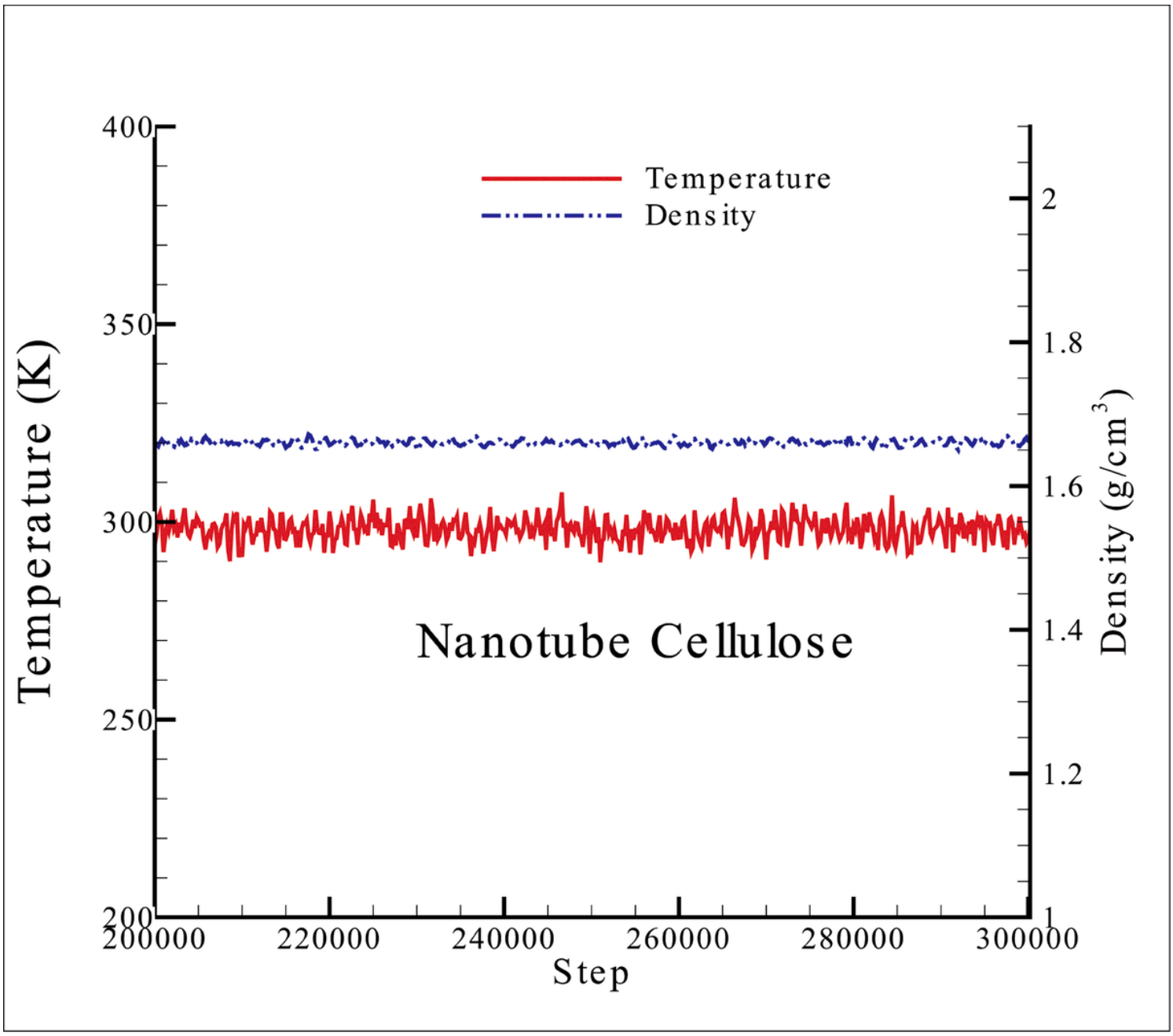

Figure 5

The simulation results of density and temperature as a function of time step are plotted for composite of CNT re-enforced cellulose.

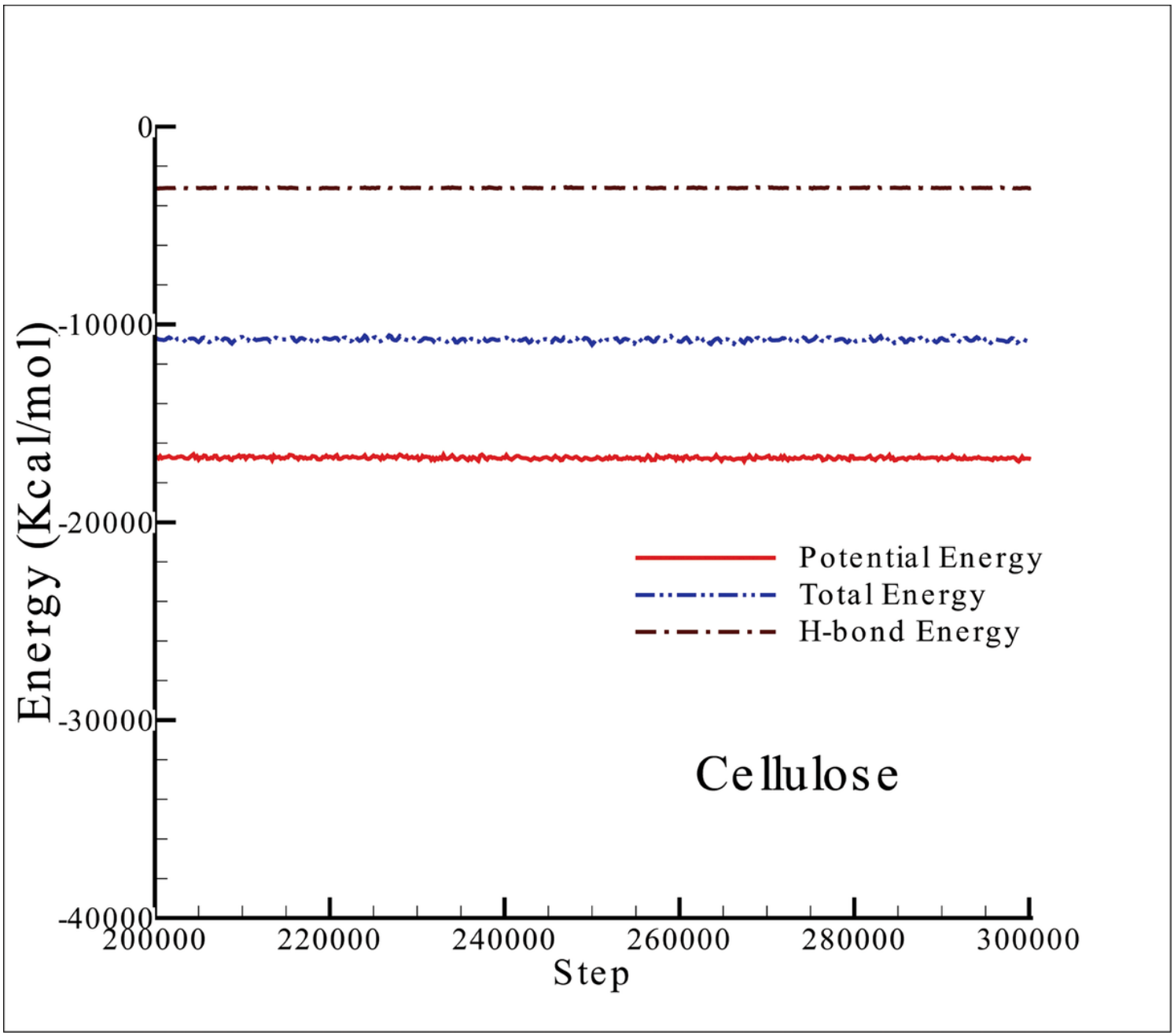

Figure 6

The results of hydrogen bond, potential, and total energies as a function of time step are plotted for I_β cellulose.

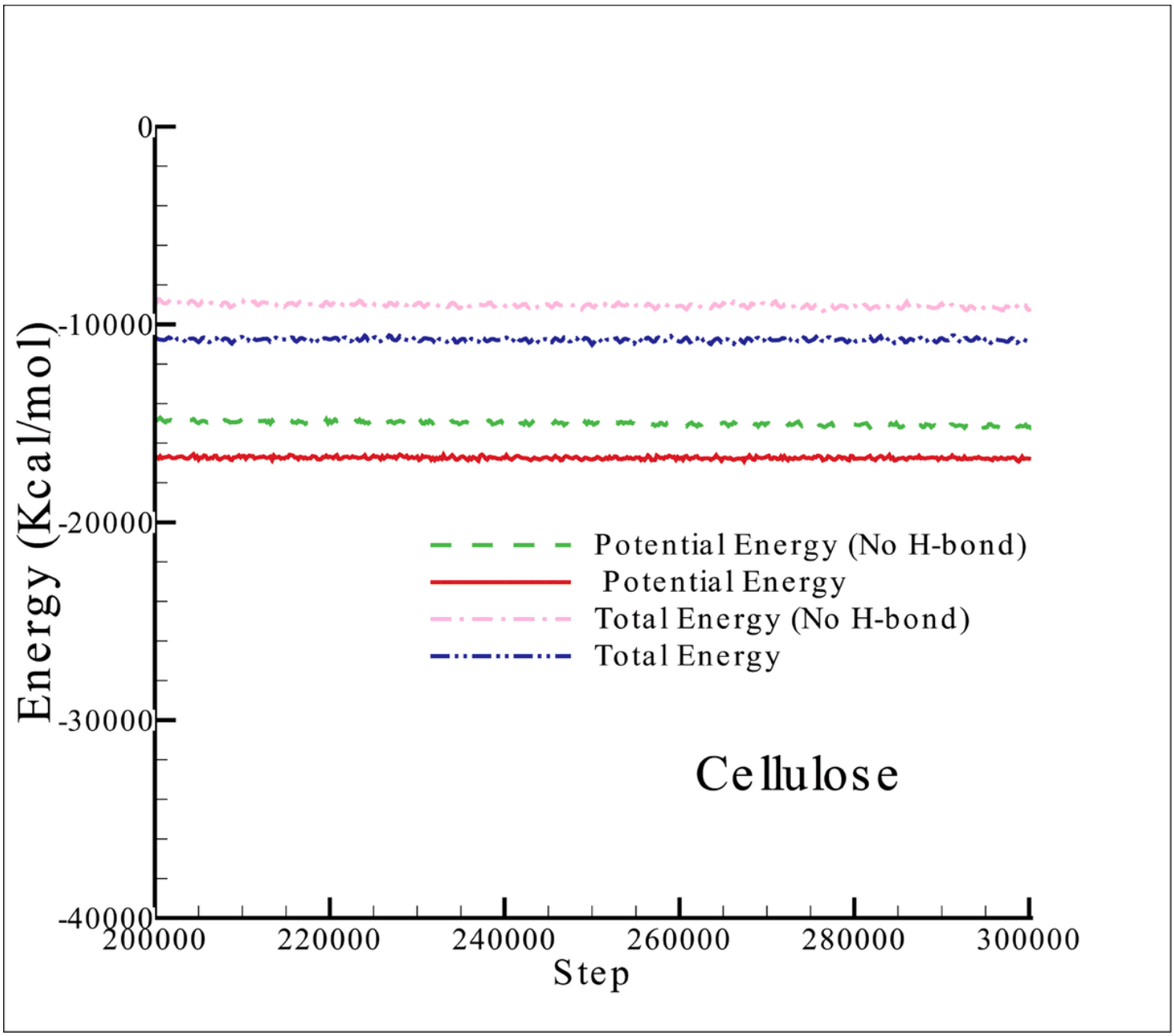

Figure 7

The simulation results of potential and total energy are compared between two cases with and without H-bonds.

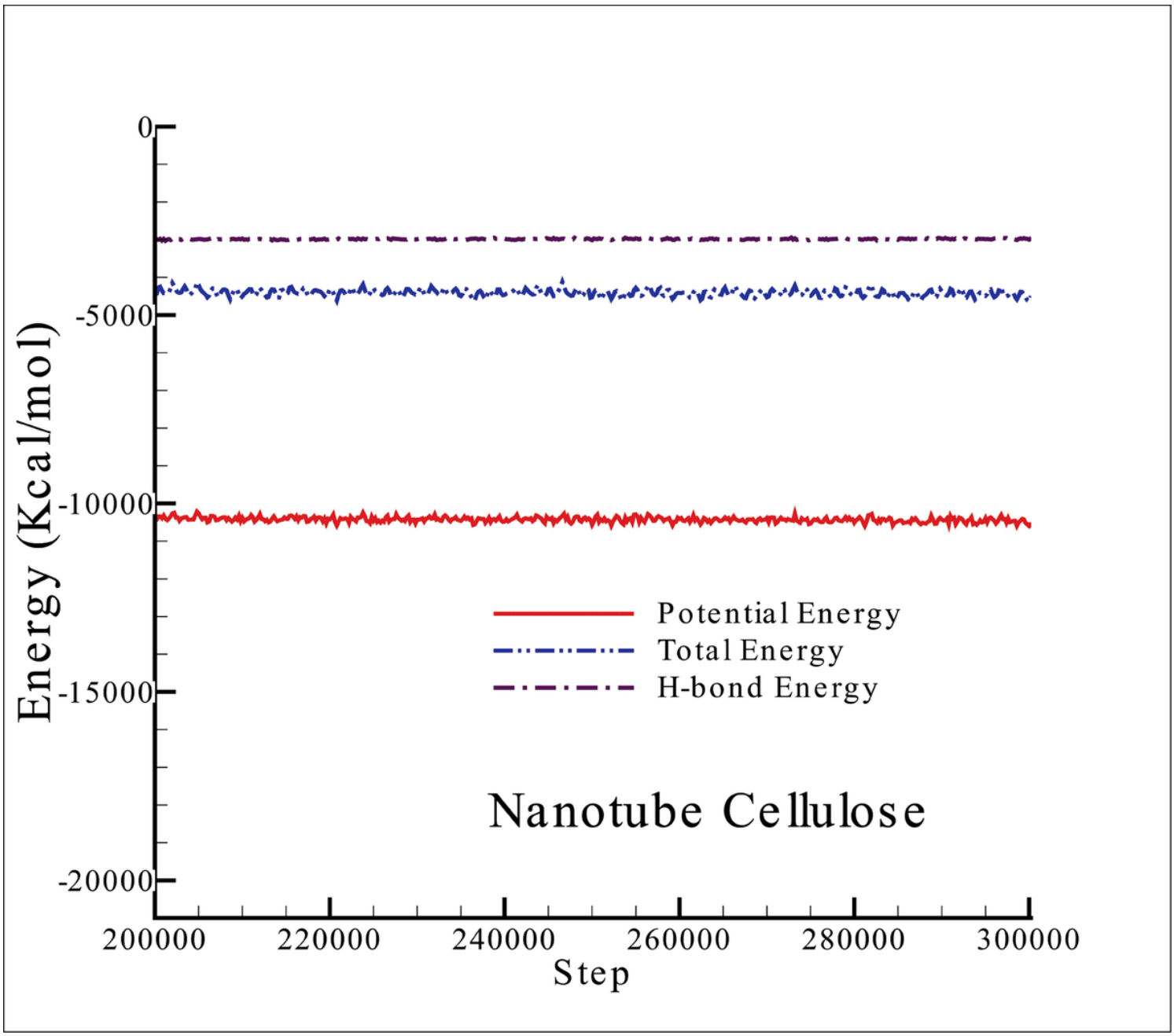

Figure 8

The results of hydrogen bond, potential, and total energies as a function of time step are plotted for composite of CNT re-enforced cellulose.

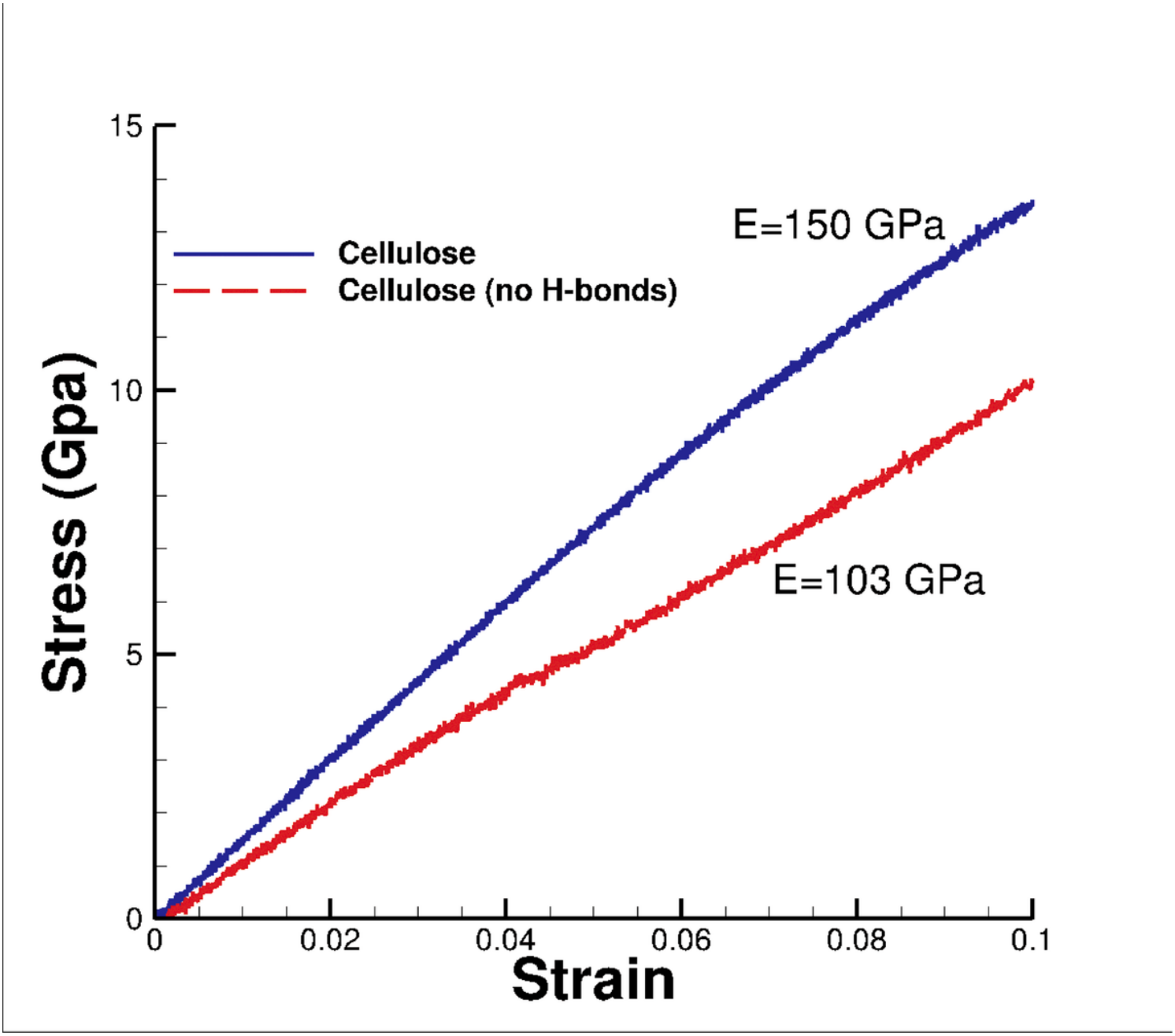

Figure 9

The stresses against strain are compared between the celluloses with and without H-bonds

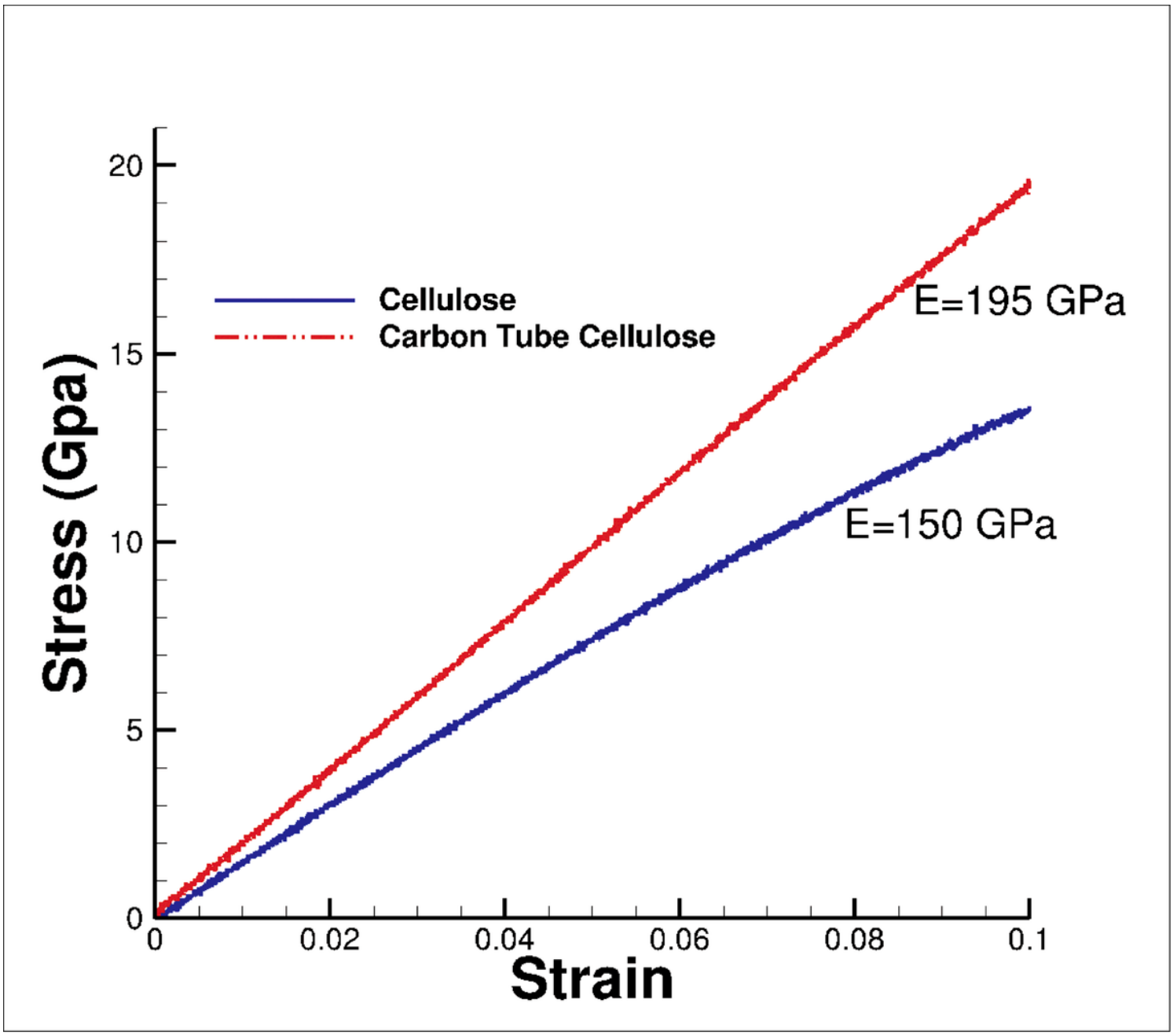

Figure 10

The simulation results of stress as a function of strain are plotted for pure cellulose crystal and composite of CNT re-enforced cellulose.